Hidden energy dissipation mechanism in nacre

Zaiwang Huang
Department of Mechanical Engineering, University of South Carolina, Columbia, South Carolina 29208, USA

Zhiliang Pan
Department of Mechanical Engineering, University of North Carolina at Charlotte, Charlotte, North Carolina 28223, USA

Haoze Li
Department of Mechanical Engineering, University of South Carolina, Columbia, South Carolina 29208, USA

Qiuming Wei[a)]
Department of Mechanical Engineering, University of North Carolina at Charlotte, Charlotte, North Carolina 28223, USA

Xiaodong Li[b)]
Department of Mechanical Engineering, University of South Carolina, Columbia, South Carolina 29208, USA; and Department of Mechanical and Aerospace Engineering, University of Virginia, Charlottesville, Virginia 22904, USA

(Received 16 March 2014; accepted 1 July 2014)

The defense mechanism that nacre (mother-of-pearl) uses to protect its living organism against high-speed predatory attack can provide lessons for engineered armor design. However, the underlying physics responsible for nacre's dynamic energy dissipation has hitherto remained a mystery to be uncovered. Here we demonstrate a new energy dissipation mechanism hidden in nacre and activated only upon dynamic loading, where the crack terminates its propagation along nacre's biopolymer interlayers but straightly impinges the aragonite platelets (95 vol%) in a transgranular manner. This intergranular–transgranular transition promotes the fracture energy dissipation, far exceeding that of the currently-used engineered ceramics. The mechanistic origin accounting for the enhancement of fracture energy dissipation is attributed to the unique nanoparticle architectured aragonite platelets. The dynamic manifestation in nacre can inspire a new route to design stronger-and-tougher engineered ceramic armors.

I. INTRODUCTION

Ceramic materials typically possess high strength and hardness but poor fracture toughness, entailing a limit for wider engineering applications. It is widely accepted that scarce plastic deformation surrounding the crack tip is primarily attributed to the notorious brittleness of the material. Upon quasi-static loading, a crack often prefers to select the grain boundary as its propagation path, whereas the grain interior remains comparatively intact. When the loading rate is boosted up to dynamic/ballistic regime, crack propagation can be diverted to cleave grain interior.[1,2] This change of crack trajectory is deemed as a so-called intergranular–transgranular transition. However, the resulting mechanical performance, i.e., compressive strength, exhibits only marginal improvement.[2] The limited mechanical enhancement in polycrystalline ceramics is attributed to the lack of plastic deformation events inside the individual grains, as evidenced by microscopic observations. Only when lateral pressure is imposed, the crack-dominated failure process will give way to the dislocation-controlled plastic deformation, accompanied with a brittle–ductile transition.

Recently, Chen et al. reported that deformation twinning can be initiated within individual alumina grains[3] when the impact pressure exceeds the Hugoniot elastic limit. The emerging plastic deformation mechanism within individual ceramic grain interiors is believed to sustain higher impact strength and inelastic strain. Yet, conversely, it is prone to become a damage source. For example, crack favors to cleaving along the twinning plane,[3] making the ceramic unavoidably brittle. Therefore, how to increase the inherent crack extension resistance from the grain interiors remains an important aspect for improving ceramics' dynamic/ballistic performance. Here we report a deformation mechanism crossover in nacre that can, on an average, stimulate 67% enhancement in compressive strength and 37-fold improvement in fracture energy dissipation, respectively when the loading rate is increased from quasi-static to dynamic range along the *c*-axis of nacre. This mechanical optimization primarily

Address all correspondence to these authors.
[a)]e-mail: qwei@uncc.edu
[b)]e-mail: xl3p@virginia.edu
DOI: 10.1557/jmr.2014.179

 © Materials Research Society 2014

https://doi.org/10.1557/jmr.2014.179 Published online by Cambridge University Press

originates from the crack trajectory conversion from the inter-platelet (along the biopolymer interlayer) to the trans-platelet (impinging the aragonite platelet). Relative to the intergranular–transgranular transition in currently-used engineered ceramics, the dynamic manifestation with an upgrading in both strength and energy dissipation in nacre is noticeably unexpected. The underlying physical origin can be ascribed to the unique nanoparticle architecture within individual aragonite platelets, where microcrack formation, rotation, and deformation of aragonite nanoparticles are collectively responsible for the inherent resistance to trans-platelet cracking. The onset of these micro-mechanisms within individual aragonite platelets is in sharp contrast to the behavior of individual grains in engineered polycrystalline ceramics. Our findings in dynamically-compressed nacre can provide an inspirational lesson for the design of stronger-and-tougher engineered ceramic armors.

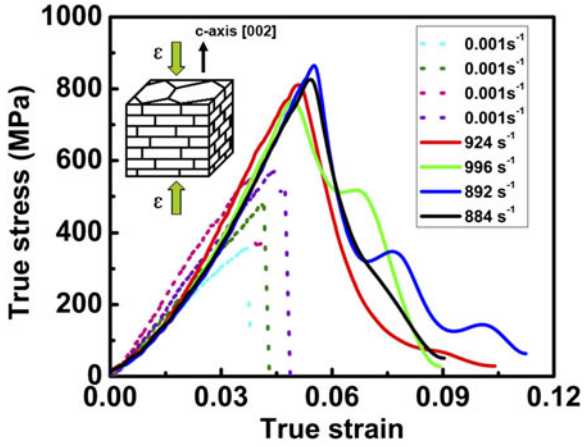


FIG. 1. True compressive stress–strain curves along nacre's *c*-axis under quasi-static and dynamic conditions, respectively. The measurement shows that maximum compressive strengths under quasi-static loading are in the spectrum of 350–580 MPa (dashed lines), lower than those (770–870 MPa) of dynamic compression (solid lines).

II. EXPERIMENTAL

In this article, natural nacre materials from California red abalone (Haliotis rufescens) that belong to the class of gastropoda were chosen for the investigation. The shells were collected alive in Santa Barbara, CA. To minimize the detrimental effect of dehydration on the structure and mechanical behavior of the shells, they were cleaned and then air delivered in ice to the laboratory where the experiments were conducted. The nacre samples were cut from the nacreous layer of the shells with a water-cooled, low-speed diamond saw. Then the nacre samples were rinsed thoroughly with distilled water. The quasi-static (sample size is 2 mm × 2 mm × 4 mm) and dynamic (sample geometry is 3 mm × 3 mm × 3 mm) uniaxial compression tests were carried out with an 810 Material test system (MTS; Eden Prairie, MN) and a Split-Hopkinson Pressure Bar (SHPB) system, respectively. The samples were pulverized upon dynamic loading. The post-mortem powders were immediately collected and dispersed in distilled water with ultrasonic wave for two hours. The powders were then transferred onto the holey carbon-coated copper grid for analysis with a JEOL JEM 2100F high-resolution transmission electron microscope (HRTEM; JEOL, Tokyo, Japan) at an accelerating voltage of 200 kV. In some regions, the sample is thin enough and suitable for HRTEM observation. Note that other techniques, i.e., ion milling, FIB can cause damage to the pristine sample, which were not used in this study.

III. RESULTS AND DISCUSSION

Figure 1 shows the true stress–strain curves upon quasi-static and dynamic compression along nacre's *c*-axis [002]. Under quasi-static loading, the compressive strength (peak strength) with a scattered character widely lies in the range of 350–580 MPa. In comparison, the dynamic compressive strength remains much more convergent, ranging from 770 to 870 MPa. Statistically, the measured strain rate sensitivity (SRS) can hit a strikingly high value, situating in the spectrum of 0.02–0.06 (Sec. 1 in Supporting materials). Microscopically, the fragment size after compression is in stark contrast upon these two loading modes. Microscopic inspection reveals that under dynamic loading the bulk nacre sample was shattered into a myriad of tiny fragments with an average size of 154 μm [Fig. 2(a)]. This severe shattering process is governed by the multicrack propagation, not by the extrusion between the compressors. The sample under quasi-static mode was, however, principally split into two parts, where the failure was driven by main-crack propagation [Fig. 2(b)], though a small amount of micrometer-sized fragmentation was found in the vicinity of the main crack. Based on these two basically different fracture mechanisms, the fracture energy dissipation ratio of the dynamic to quasi-static loading was estimated to be 37 (Sec. 2 in Supporting materials). The striking manifestation with a simultaneous improvement in both strength and fracture energy dissipation is fascinating for its application as a natural body armor against predatory attack.[4] Yet, the underlying physical mechanism of how nacre optimizes dynamic energy dissipation still remains a mystery to be uncovered.

A close-up fractography observation on the individual fragments indicates that the dynamic crack trajectory was mostly governed by the trans-platelet penetration [Fig. 2(c)] vis-à-vis the inter-platelet crack deflection [Fig. 2(d)] under quasi-static compression. It is well known that under uniaxial compression, brittle solids[5] fail by cracking along the compression direction, which has been rationalized by the wing-type crack model involving the main crack nucleation and alignment, and

https://doi.org/10.1557/jmr.2014.179 Published online by Cambridge University Press

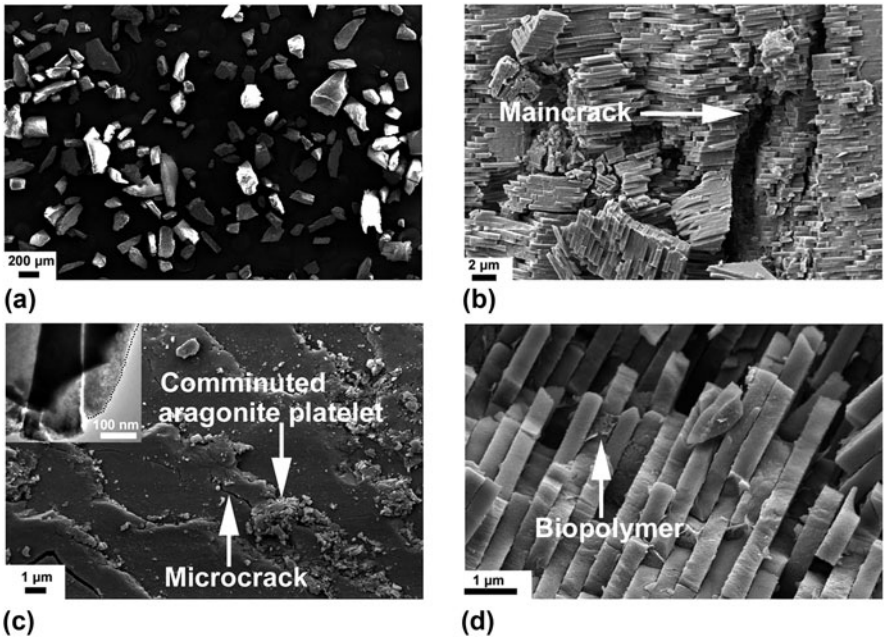


FIG. 2. Competition of trans-platelet and inter-platelet fracture upon dynamic and quasi-static compression. (a) Bulk sample has been shattered into fragments ranging from submillimeter to nanometer, in sharply contrast with that under quasi-static condition (b). (c) A closer examination on dynamic individual fragment shows that advancing crack impinges the aragonite platelet in a transgranular manner, unlike the inter-granular crack propagation under quasi-static loading. (d) Compared with the trans-platelet fracture, crack picks up biopolymer interlayers as its propagation pathways under quasi-static compression, where the biopolymer can be clearly seen (white arrowed).

then coalescence of randomly-distributed small cracks. Owing to the much lower elastic modulus compared with the ceramic aragonite, the biopolymer interlayers parallel to the *c*-axis can be readily activated as the crack initiation sites under quasi-static condition. These microcracks will experience nucleation, growth, interaction, coalescence and will ultimately lead to failure. Of noteworthy importance is that the failure path is, macroscopically, toward the *c*-axis. Yet, microscopically, it actually lies along the biopolymer interface [Fig. 2(d)] in a zigzag fashion. One may ask why there exists a crossover between trans-platelet and inter-platelet fracture modes. The critical competition condition whether a crack chooses inter-platelet or trans-platelet fracture can be described as follows[6,7]:

$$\frac{G_{\mathrm{Trans}}}{G_{\mathrm{Inter}}} = \frac{\Gamma_{\mathrm{AP}}}{\Gamma_{\mathrm{Bio}}} \quad , \tag{1}$$

where G_{Trans}, G_{Inter}, Γ_{AP}, Γ_{Bio} are the energy release rates of the trans-platelet crack tip and the inter-platelet crack tip, the fracture toughness of the aragonite platelet and the biopolymer interlayer, respectively. Here we notice that no specific toughness values for the biopolymer and the aragonite platelets can be currently acquired. He and Hutchinson[7] developed a model to evaluate the conversion of inter-platelet [Fig. 3(a)] and trans-platelet [Fig. 3(b)] crack ($G_{\mathrm{Inter}}/G_{\mathrm{Trans}}$) through introducing Dundurs' parameter[8] $\alpha = (E_{\mathrm{AP}} - E_{\mathrm{Bio}}/E_{\mathrm{AP}} + E_{\mathrm{Bio}})$. Previous studies reported that the elastic modulus of the aragonite platelet and the biopolymer interlayer are 70 GPa[9] and 10 GPa,[10] respectively. Thus, the value of Dundurs' parameter α is ~0.75 and the corresponding critical ratio ($G_{\mathrm{Inter}}/G_{\mathrm{Trans}}$) approaches ~0.92[7] [Fig. 3(c)]. Then, we can try to find the critical energy release ratio under dynamic loading condition. A recent dynamic compression study on amorphous biopolymer[11] showed that the improved amount of toughness can reach 20%. As for the nanoparticle-structured aragonite platelet, we consider it as a composite with the same chemistry arrangement (aragonite and biopolymer) as nacre, referring to 37-fold improvement in fracture energy dissipation. As derived from this, the energy release ratio is $G_{\mathrm{Inter}} \leq 0.03 G_{\mathrm{Trans}}$. This means that the propensity of trans-platelet processes increases by raising the strain rate [Fig. 3(c)]. Note that He–Hutchinson mode[6] can be only applied to linear-elastic materials. The compression behavior of biopolymer in nacre is not strictly in the range of elasticity. However, the volume fraction of biopolymer is only 5% and under dynamic loading the polymer behavior can be changed to be "rigid" owing to the extremely short loading time span. When the compression is loading along the *c*-axis of nacre, the crack transition from previous interface to impinging the platelet directly can be explained by the He–Hutchinson mode.[6] From this mode, only one-point value can be measured for quasi-static and dynamic compression, respectively, for $G_{\mathrm{Inter}}/G_{\mathrm{Trans}} = 0.03$ when $\alpha = 0.75$ for quasi-static compression, $G_{\mathrm{Inter}}/G_{\mathrm{Trans}} = 0.92$ when $\alpha = 0.75$. One single point cannot derive the exact

https://doi.org/10.1557/jmr.2014.179 Published online by Cambridge University Press

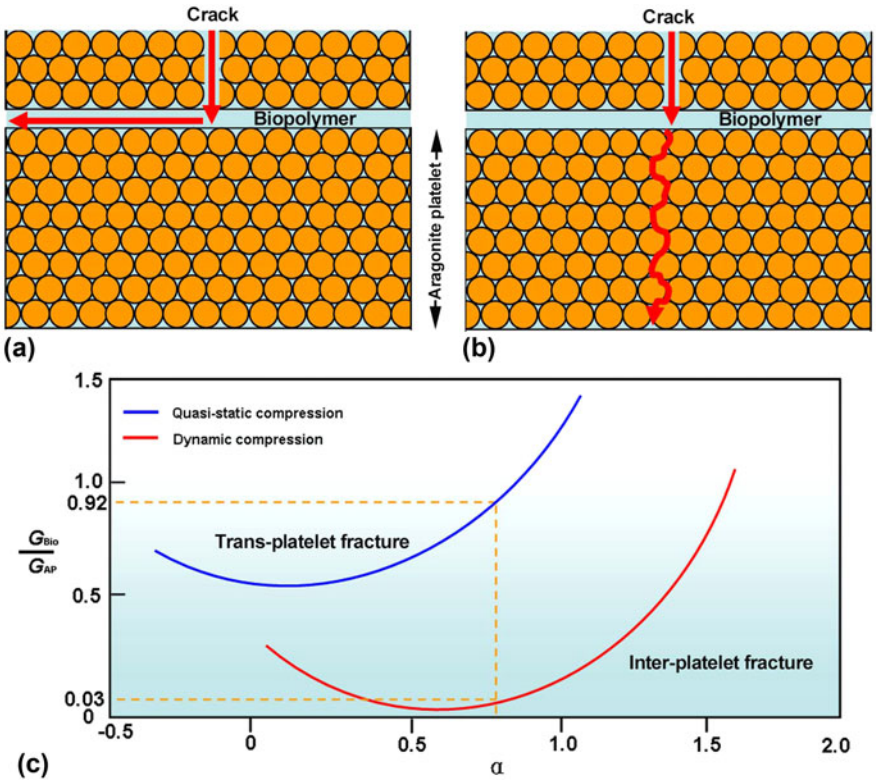


FIG. 3. Inter-platelet to trans-platelet fracture transition from quasi-static to dynamic compression. (a) Crack prefers to nucleate and propagate along the biopolymer interface under quasi-static compression. (b) Upon dynamic loading, crack has limited time to pick up the soft interface, but impinges the aragonite platelet in a cleave manner. (c) Linear elasticity solution based on He–Hutchinson[7] shows that the ratio of strain energy release rate ($G_{\text{Inter}}/G_{\text{Trans}}$) is equal to 0.92 under quasi-static compression, but this value can be reduced to 0.03 upon dynamic background. This value means that the propensity of trans-platelet fracture will be considerably increased.

curve, and only the trend of the curve is illustratively demonstrated to explain the possible mechanism.

Furthermore, we found that the details of the dynamic processes within individual aragonite platelets are strikingly unexpected. As discussed above, the dynamic crack can invade the aragonite platelets because of high strain energy release rate at the crack tip. Figure 2(c) shows that the geometrically regular polygonal aragonite platelets have been shattered in a jagged manner (inset). Simultaneously, zigzag microcrack formation and nanoscale fragmentation within aragonite platelets are believed to account for two remarkable energy dissipation mechanisms. In engineered ceramic materials, transgranular crack often cleaves the grain interiors, but leaves a smooth fracture surface, where rare plastic deformation can be associated with the crack propagation process.[2] Considering that the individual aragonite platelets have been long regarded as single-crystal ceramic mineral, the occurrence of the zigzag microcracks and nanoscale fractured debris is unique for energy absorption, pointing toward the inherent microstructure resistance against dynamic trans-platelet crack. In contrast, the quasi-static fractography displays that crack propagation was along the biopolymer interface [Fig. 2(d)] while most of aragonite platelets remain comparatively intact. Therefore, this unusual behavior of the aragonite platelets implies its unique structural composition and dynamic crack resistance for enhancing energy dissipation. The working mechanism responsible for deformation, in particular, for defeating dynamic crack propagation, remains to be further elaborated on.

Upon quasi-static compression, the plastic deformation of aragonite platelets arises from the remote compressive stress field. From our previous results, the compressive stress can lead to rotation/reorientation of aragonite nanoparticles from the previously prevalent inter-parallel manner.[12] This inter-nanoparticle mechanism is mainly a result of the extremely small particle size (a few nanometers), which suppresses the plastic deformation from the grain interior.[13] In comparison, the atomistic observation [Fig. 4(a)] from the dynamically-compressed debris (directly collected from the post-mortem fragments) reveals that the lattice imperfection within individual aragonite nanoparticles can be provoked, aside from nanoparticle rotation based on the ring-like diffraction pattern [inset in Fig. 4(a)]. Careful atom-to-atom measurement [Fig. 4(b)] reveals that the atomic sequence (marked by the red line) has suffered from debonding (marked by

https://doi.org/10.1557/jmr.2014.179 Published online by Cambridge University Press

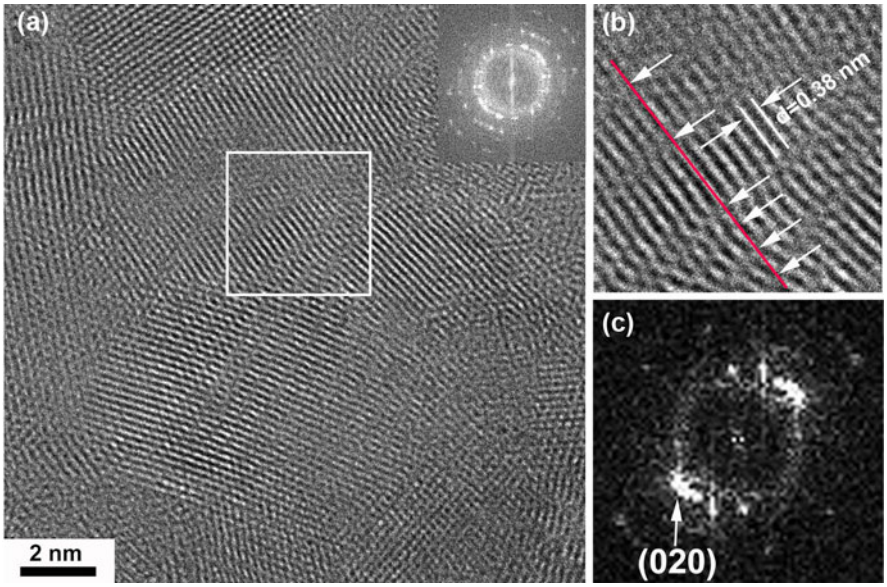


FIG. 4. Amorphization of crystalline aragonite nanoparticles under dynamic compression. (a) The highly-oriented aragonite nanoparticles have been re-organized in a disordered manner after dynamic compression (inset). (b) A close-up view shows that amorphization is provoked within individual aragonite nanoparticles by means of atom-to-atom measurement, where the aligned atomic ordering (red line) undergoes debonding/deflection at least six times (white arrowed). (c) Corresponding FFT pattern with a messy character is consistent with the amorphization.

white arrows) at least six times. The resultant atomic configuration in a disorganized manner [Fig. 4(c)] within individual aragonite nanoparticles can be regarded as neither simple lattice dislocations nor other well-known defect types such as twinning, or stacking faults. In view of the disordered atom arrangement, we take this lattice imperfection as amorphization. The atomic origin of transition from crystalline state to amorphous state probably stems from the depressurization (pressure quenching).[14] The high energy release rate at the dynamic crack tip makes it possible for aragonite nanoparticles to encounter a sudden pressure release. This depressurization process can induce localized atomic lattice bending, represented by atom rearrangement. Alternatively, it is also possible that the localized shear stress[1,15] arising from the trans-platelet crack can provoke amorphization. The extremely high energy release rate at the crack tip renders the possibility to cleave the aragonite nanoparticles, where the atomic pattern associated with amorphization will be reorganized at the newly-formed crack surface. In this regard, the trans-platelet dynamic crack can initiate trans-nanoparticle amorphization, contrary to the inter-nanoparticle rotation under quasi-static condition.

In thermodynamics, a quantitative evaluation of trans-nanoparticle amorphization can be considered based on the plastic deformation activation volume (v^*)[16]

$$v^* = \frac{\sqrt{3} \cdot k \cdot T}{\sigma \cdot m} \quad , \qquad (2)$$

here k is the Boltzmann constant (1.38×10^{-23} m^2 kg s^{-2} K^{-1}), T is the absolute temperature, and σ and m are the effective stress and the SRS, respectively. The activation volume, v^*, is a measure of the physical domain activated during a plastic deformation event, or the plastic deformation sampling volume. The measured activation volume under dynamic loading is estimated to be approximately a few b^3 (Sec. 1 in supporting materials. b is the magnitude of the Burgers vector of the lattice dislocation). This value means that the plastic activation source can be highly confined within an extremely small dimension. Our previous study[17] has shown that the onset of partial dislocation and deformation twinning within individual aragonite nanoparticles can be related to the tiny activation volume (a few b^3) when loaded along nacre's cross section. We suggest that the debut of amorphization indeed corresponds to a higher stress level to be initiated relative to the partial dislocation and deformation twinning. The amorphization process involves rearrangement of the atomic or molecular ensemble, whereas the onset of partial dislocations and deformation twinning only implicates the motion and/or replacement of several-layer atoms.[18] In general, only when the relatively "easier" mechanisms, such as (partial) dislocation, stacking fault, twinning, cannot be sustained to carry the plastic deformation, is it then compulsory to trigger atomic disordering to accommodate the extremely high stress and energy concentration. It should be pointed that the activation volume under quasi-static loading is measured to be approximately 18 b^3 (see Sec. 1 in supporting materials), which is much higher than that obtained from the counterpart of under dynamic loading. The difference can be reasonably related to the mechanistic transition from inter-nanoparticle (rotation) to trans-nanoparticle (amorphization), but is

https://doi.org/10.1557/jmr.2014.179 Published online by Cambridge University Press

not simply related to the intergranular–transgranular crack trajectory transition.

Interestingly, then, we can inquire: why can the amorphization processes be frequently provoked along nacre's *c*-axis, contrary to the onset of partial dislocation and deformation twinning from the cross section? The difference comes from the orthotropic structural architecture in nacre,[19] where the geometrically interlaced arrangement of the aragonite platelets viewed from the *c*-axis enables crack propagation at a higher stress level relative to propagation from the cross section.[2] This conclusion is in excellent agreement with the fractography (Sec. 3 in Supporting materials) that the fragment size distribution under dynamic compression along the cross section far exceeds that loaded along the *c*-axis, and wherein, the crack readily forms and propagates at a comparatively low stress level in view of the structure feature of conjoint biopolymer interfaces loaded from the cross section (Sec. 4 in Supporting materials). For *c*-axis, the geometrically staggered arrangement of aragonite platelets hinders crack propagation and requires comparatively high stress level to be cleaved.

IV. CONCLUSIONS

Nature's wisdom in nacre resides in its unique hierarchical structure that renders nacre an exceptional energy dissipation mechanism for protecting its living organism against high-speed predatory attack. The fracture energy upon dynamic compression is 37-fold higher than that of quasi-static compression. The activation volume derived from dynamic deformation is extremely localized, leading to the interior amorphization of individual aragonite nanoparticle. The dynamic manifestation of nacre should receive intense attention and the lesson learned from nacre can thus inspire us to design stronger-and-tougher ceramic armors through multiscale structuring.

ACKNOWLEDGMENTS

We thank the help from D. Wilhelm for compression test. We also appreciate the help with SEM and TEM observation from Y.C. Yang and D. Blom, respectively. This work was supported by the U.S. Army research office under agreement/Grant No. W911 NF-07-1-0449. Q.M. Wei was grateful for the financial support of U.S. Army Research Office under Grant No. W911NF-07-1-0335.

REFERENCES

1. G. Hu, K.T. Ramesh, B. Cao, and J.W. McCauley: The compressive failure of aluminum nitride considered as a model advanced ceramic. *J. Mech. Phys. Solids* **59**(5), 1076 (2011).
2. G. Hu, C.Q. Chen, K.T. Ramesh, and J.W. McCauley: Mechanisms of dynamic deformation and dynamic failure in aluminum nitride. *Acta Mater.* **60**(8), 3480 (2012).
3. M.W. Chen, J.W. McCauley, D.P. Dandekar, and N.K. Bourne: Dynamic plasticity and failure of high-purity alumina under shock loading. *Nat. Mater.* **5**(8), 614 (2006).
4. F. Barthelat, H. Tang, P.D. Zavattieri, C.M. Li, and H.D. Espinosa: On the mechanics of mother-of-pearl: A key feature in the material hierarchical structure. *J. Mech. Phys. Solids* **55**(2), 306 (2007).
5. M.F. Ashby and S.D. Hallam: The failure of brittle solids containing small cracks under compressive stress states. *Acta Metall. Mater.* **34**(3), 497 (1986).
6. J.W. Hutchinson and Z. Suo: Mixed-mode cracking in layered materials. *Adv. Appl. Mech.* **29**, 63 (1992).
7. M.Y. He and J.W. Hutchinson: Crack deflection at an interface between dissimilar elastic-materials. *Int. J. Solids Struct.* **25**(9), 1053 (1989).
8. J. Dundurs and D.B. Bogy: Edge-bonded dissimilar orthogonal elastic wedges under normal and shear loading. *J. Appl. Mech.* **36**(3), 650 (1969).
9. Z. Huang and X. Li: Nanoscale structural and mechanical characterization of heat treated nacre. *Mater. Sci. Eng., C* **29**(6), 1803 (2009).
10. Z-H. Xu, Y. Yang, Z. Huang, and X. Li: Elastic modulus of biopolymer matrix in nacre measured using coupled atomic force microscopy bending and inverse finite element techniques. *Mater. Sci. Eng., C* **31**(8), 1852 (2011).
11. V. Prakash and N. Mehta: Uniaxial compression and combined compression-and-shear response of amorphous polycarbonate at high loading rates. *Polym. Eng. Sci.* **52**(6), 1217 (2012).
12. X. Li and Z. Huang: Unveiling the formation mechanism of pseudo-single-crystal aragonite platelets in nacre. *Phys. Rev. Lett.* **102**(7), 075502 (2009).
13. Z.W. Shan, E.A. Stach, J.M.K. Wiezorek, J.A. Knapp, D.M. Follstaedt, and S.X. Mao: Grain boundary-mediated plasticity in nanocrystalline nickel. *Science* **305**(5684), 654 (2004).
14. X.Q. Yan, Z. Tang, L. Zhang, J.J. Guo, C.Q. Jin, Y. Zhang, T. Goto, J.W. McCauley, and M.W. Chen: Depressurization amorphization of single-crystal boron carbide. *Phys. Rev. Lett.* **102**(7), 075505 (2009).
15. D. Ge, V. Domnich, T. Juliano, E.A. Stach, and Y. Gogotsi: Structural damage in boron carbide under contact loading. *Acta Mater.* **52**(13), 3921 (2004).
16. Q. Wei: Strain rate effects in the ultrafine grain and nanocrystalline regimes—its influence on some constitutive behavior. *J. Mater. Sci.* **42**, 1709 (2007).
17. Z. Huang, H. Li, Z. Pan, Q. Wei, Y.J. Chao, and X. Li: Uncovering high-strain rate protection mechanism in nacre. *Sci. Rep.* **1**(148), 148 (2011).
18. V. Yamakov, D. Wolf, S.R. Phillpot, A.K. Mukherjee, and H. Gleiter: Dislocation processes in the deformation of nanocrystalline aluminium by molecular-dynamics simulation. *Nat. Mater.* **1**(1), 45 (2002).
19. J.D. Currey: Mechanical-properties of mother of pearl in tension. *Proc. R. Soc. London Ser. B* **196**(1125), 443 (1977).

Supplementary Material

To view supplementary material for this article, please visit http://dx.doi.org/jmr.2014.179.

https://doi.org/10.1557/jmr.2014.179 Published online by Cambridge University Press